CHARACTERIZATION OF HIGH Ge CONTENT SiGe HETEROSTRUCTURES AND GRADED ALLOY LAYERS USING SPECTROSCOPIC ELLIPSOMETRY

A. R. Heyd*,†, S. A. Alterovitz*, and E. T. Croke‡

*NASA Lewis Research Center, 21000 Brookpark Road, MS 54-5, Cleveland, OH 44135

‡Hughes Research Laboratories, 3011 Malibu Canyon Rd, MS RL63, Malibu, CA 90265

†This work was performed while the author held a National Research Council-NASA Research Associateship

ABSTRACT

Si_xGe_{1-x} heterostructures on Si substrates have been widely studied due to the maturity of Si technology. However, work on Si_xGe_{1-x} heterostructures on Ge substrates has not received much attention. A Si_xGe_{1-x} layer on a Si substrate is under compressive strain while Si_xGe_{1-x} on Ge is under tensile strain; thus the critical points will behave differently. In order to accurately characterize high Ge content Si_xGe_{1-x} layers the energy shift algorithm, which is used to calculate alloy compositions, has been modified. These results have been used along with variable angle spectroscopic ellipsometry (VASE) measurements to characterize Si_xGe_{1-x}/Ge superlattices grown on Ge substrates. The results are found to agree closely with high resolution x-ray diffraction measurements made on the same samples.

The modified energy shift algorithm also allows the VASE analysis to be upgraded in order to characterize linearly graded layers. In this work VASE has been used to characterize graded Si_xGe_{1-x} layers in terms of the total thickness, and the start and end alloy composition. Results are presented for a 1 μm Si_xGe_{1-x} layer linearly graded in the range $0.5 \leq x \leq 1.0$.

INTRODUCTION

Si_xGe_{1-x}/Si epilayers have recently started to be used for device fabrication. The ability to vary the Si composition, x, in the Si_xGe_{1-x} layer offers the device designer a wide range of options. To date, most work has been focused on Si_xGe_{1-x}/Si heterostructures grown on Si substrates. To our knowledge little work has been done on high Ge content Si_xGe_{1-x} structures grown on Ge substrates. The ability to deposit quality Si_xGe_{1-x}/Ge heterostructures will further expand the material properties and band offsets available to device engineers. As interest in high Ge content Si_xGe_{1-x} materials increases, accurate characterization techniques of such materials and structures will be needed.

Recently, variable angle spectroscopic ellipsometry (VASE) has been shown to be a powerful, non-destructive technique for the post-deposition characterization of Si_xGe_{1-x}/Si superlattices (SLs) and device structures [1,2]. In these studies VASE was used to determine the layer thicknesses, alloy composition, oxide thickness, sample homogeneity, and number of SL periods. The alloy composition was determined by interpolating between the Si_xGe_{1-x} dielectric functions of Jellison *et al.* [3]. However, only the Si rich materials, $x > 0.5$, were considered. In this current work, we have turned our attention to high Ge content Si_xGe_{1-x}/Ge SLs grown on Ge substrates. To accomplish this, the Si_xGe_{1-x} interpolation scheme has been modified so that it can be used for Si_xGe_{1-x} at all compositions, $0.0 \leq x \leq 1.0$.

In order to relieve stress in Si_xGe_{1-x} layers, a graded layer is typically grown on the substrate. Graded alloy layers can also be found in the base of heterojunction bipolar transistors (HBT) structures. In the past, to characterize structures which contain a graded alloy buffer by VASE, the low energy portion of the spectra was ignored, thus ensuring that the graded buffer would not affect the analysis. To improve the VASE analysis of structures containing graded buffers and to

Mat. Res. Soc. Symp. Proc. Vol. 358 ©1995 Materials Research Society

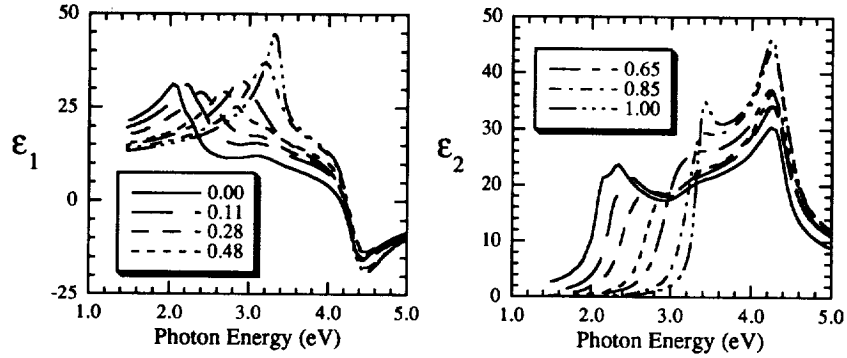

Figure 1: The Si_xGe_{1-x} dielectric functions of Ref. 3. The dielectric functions for $x > 0.5$ and $x < 0.5$ were determined from thick Si_xGe_{1-x} layers on Si and Ge substrates respectively. The spectra for $x = 0.2$, 0.47, and 0.98 have been omitted for clarity.

enable the characterization of graded bases, the analysis software has been updated to account for graded alloy layers with an arbitrary alloy profile.

EXPERIMENTAL DETAILS

All materials used in this study were grown using a Perkin-Elmer (Model 430S) Si MBE system. Deposition of Si and Ge took place in an ultrahigh vacuum (base pressure $< 1 \times 10^{-10}$ Torr) from dual e-beam evaporation sources onto rotating Si or Ge (100) substrates. After deposition, a rotating analyzer ellipsometer was used to record the ellipsometric parameters, $\{\tan\Psi, \cos\Delta\}$, over the spectral range 300–800 nm. All samples were measured at several angles of incidence chosen to increase the sensitivity of the ellipsometric angles to the structure parameters [4]. The SL structures were also measured by high-resolution x-ray diffraction (HRXRD) which directly determines the thickness and average Si content of one period [5,6]. The thickness and composition of the individual SL layers can be calculated from the period, average Si content, and knowledge of the shutter opening/closing times from the growth log.

The energy shift algorithm [7] is used to interpolate between the Si_xGe_{1-x} dielectric functions which are given at a number of fixed x values [3,8]. This algorithm requires that the location of each critical point (CP) be expressed as a function of the Si content, x. Previous studies of high Si content Si_xGe_{1-x}/Si heterostructures [1,2,9–11] have used the functional forms of three CPs ($E_o(x)$, $E_1(x)$, and $E_2(x)$) in the analysis. The energy shift algorithm has been modified for this study in order to account for four CPs by adding the change in the $E_1 + \Delta_1$ CP with composition. The $E_1 + \Delta_1$ CP has little effect in the energy shift algorithm for relaxed, high Si content Si_xGe_{1-x} where the splitting is small, $\Delta_1 \cong 0.029$ at $x = 1.0$ [12]. The $E_1 + \Delta_1$ CP function has more of an effect for low Si content and strained Si_xGe_{1-x} structures where the splitting is much greater.

The Si_xGe_{1-x} data base of Ref. 3, shown in Fig. 1, has been chosen for this work over the data base of Ref. 8 due to its more accurately determined compositions, and wider spectral range particularly in the infrared as discussed in Ref. 1. The Si_xGe_{1-x} dielectric functions were determined by spectroscopic ellipsometry from thick Si_xGe_{1-x} layers ($d \sim 8\mu$m) on Si substrates for x = 98%, 85%, 65%, 47% and on Ge substrates for x = 48%, 28%, 20%, 11%. The E_1, $E_1 + \Delta_1$ and E_2 CP functions, shown in Fig. 2, were determined through a CP analysis [12] of the Si_xGe_{1-x} dielectric functions. The resolution of the published Si_xGe_{1-x} data is not sufficient to

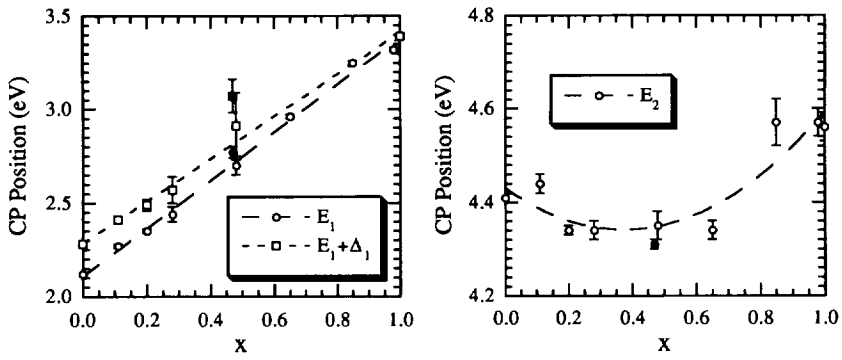

Figure 2: E_1, $E_1 + \Delta_1$, and E_2 critical points energies calculated from the Si_xGe_{1-x} dielectric functions of Ref. 3. The CPs determined for $Si_{0.47}Ge_{0.53}$ are displayed as solid symbols and were not used to determine the best fit lines.

resolve the E_1 and the $E_1 + \Delta_1$ CPs for $x > 0.5$, so only the E_1 CP is considered in this region. The dielectric functions for $x = 47\%$ and 48% (on Si and Ge substrates, respectively) are quite different [3] and lead to inconsistencies in the CP analysis. It can be seen from Fig. 2 that the CP energies calculated for $x = 47\%$ deviate the greatest from the overall best fit line, and have therefore been omitted in the analysis. The CP functions determined from the curves in Fig. 2 are:

$$\begin{aligned} E_1 &= 2.11 + 1.28x \\ E_1 + \Delta_1 &= 2.28 + 1.13x \\ E_2 &= 4.31 - 0.261x + 0.228x^2 \quad . \end{aligned} \tag{1}$$

As $E_o(x)$ is not an important function in the algorithm, it has been approximated by a linear interpolation between the fundamental indirect band gaps of silicon and germanium [13]:

$$E_o = 0.68 + 0.44x \quad . \tag{2}$$

Strain dependence was neglected through all the algorithm calculations for two reasons: strain effects on the CP were calculated [10, 14] and found to be very small, and no reference dielectric functions for strained Si_xGe_{1-x} are available for high Ge concentrations. In addition, measurement of such functions is very complicated as the coherently strained calibration samples have to be thinner than the critical thickness.

RESULTS AND DISCUSSION

Si_xGe_{1-x}/Ge superlattice structures

Two twenty period Si_xGe_{1-x}/Ge SL structures, labeled A and B, were grown on Ge substrates. The target parameters for one period are shown in Table I along with the HRXRD results.

Each sample was measured using VASE at angles of incidence of 69°, 73°, and 77°. The VASE data for Sample A are shown in Fig. 3. To analyze the VASE data a model is generated which assumes each layer to be homogeneous and isotropic and all interfaces to be abrupt. In addition, each period of the SL is assumed to be identical in terms of both the thicknesses and optical

Table I: Comparison of target sample structure with that determined by HRXRD and VASE. The period is the sum of the Ge and SiGe layer thicknesses, and x(avg) is the average silicon content in one period. The parameters of the VASE analysis are the oxide, Ge, and SiGe layer thicknesses, and the silicon content, x, of the SiGe layer.

Sample	Source	Period (Å)	x(avg) (%)	d(Ge) (Å)	d(SiGe) (Å)	x (%)
A	target	178.0	6.2	128	50	22
A	HRXRD	201.1	8.0	141.8	59.3	26.6
A	VASE[a]	202.8	8.4	127.5 ± 3.9	75.3 ± 3.5	22.7 ± 1.6
B	target	201.0	7.8	142	59	26.6
B	HRXRD	202.1	8.3	141.8	60.3	27.5
B	VASE[b]	204.5	8.4	126.9 ± 4.7	77.6 ± 4.4	22.1 ± 2.0

[a] σ = 0.0137 and d(oxide) = 17.9 Å ± 0.4 Å.
[b] σ = 0.0167 and d(oxide) = 25.5 Å ± 0.6 Å.

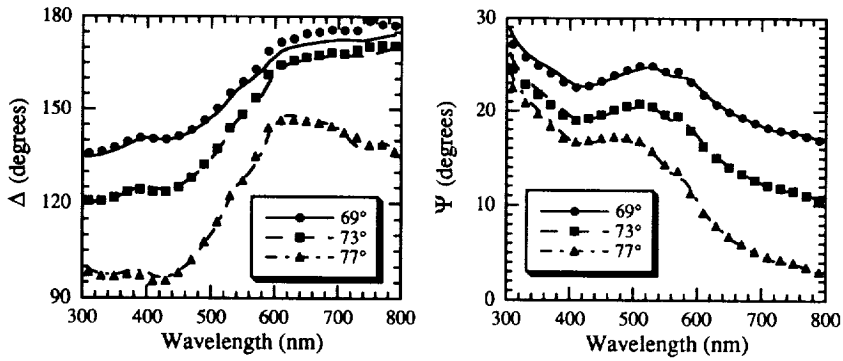

Figure 3: Comparison of measured VASE data for Si_xGe_{1-x}/Ge SL sample A with the ellipsometric spectra determined from the best fit model. The symbols represent the measured data and the lines represent the data calculated from the model. Sample B show similar fitting.

properties. The native oxide has been simulated using the dielectric function for GeO_2 taken from the literature [15]. The results of the VASE analysis are shown in Table I; the period and average Si content were calculated from the individual layer thicknesses and x.

The agreement between the HRXRD and the VASE results are excellent when comparing the period and x(avg). The individual layer thicknesses and x, however, differ quite a bit. The {Δ, Ψ} spectra generated from the model are shown in Fig. 3 as dashed lines. The fit can be seen to be quite good, especially in the Ψ spectra. The poor fitting in the long wavelength region of the 69° and 73° Δ spectra is due to the inability of a rotating element ellipsometer to accurately determine Δ values near 0° and 180°. Some small oscillations in Δ can also be seen in the long wavelength region which are not reproduced by the model. In this region the optical penetration depth is large and the model is sampling the entire structure. These results suggest that the periods are not identical in terms of thickness and/or x(avg) as is assumed in the model. This may in some part be responsible for the discrepancies in the individual thicknesses and x. Further work is necessary to determine the exact nature of these discrepancies which may also be attributed to

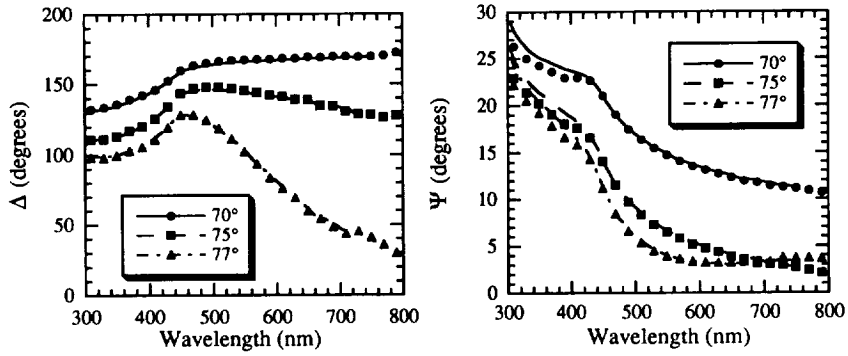

Figure 4: Ellipsometric data on graded Si_xGe_{1-x} layers. The experimental data are shown as symbols and the best fit model is shown as dashed lines.

non-uniformities within a single period as a result of a) fluctuations in the Si content of a single Si_xGe_{1-x} layer or b) interfacial layers.

Si_xGe_{1-x} graded layer

Finally, a 1 μm graded Si_xGe_{1-x} layer was grown on a Si substrate. The layer is linearly graded from $x = 1.0$ to 0.5. The sample was measured by VASE at 70°, 75°, and 77°. The measured spectra are shown in Fig. 4. To model the graded layer the total thickness is divided into $n + 1$ ($n > 0$) layers each of thickness d_i and Si content x_i. The i-th ($0 \leq i \leq n$) layer thickness is given by:

$$d_i = \begin{cases} D/2n & i = 0, n \\ D/n & 1 \leq i < n \end{cases} \tag{3}$$

where D is the total layer thickness. The alloy content is assumed to vary linearly between x_0 and x_n,

$$x_i = \frac{(n-i)x_0 + ix_n}{n} \quad . \tag{4}$$

In theory this model will approximate a linear continuously graded layer exactly as $n \rightarrow \infty$ although for the graded sample used in this work values of $n > 20$ yield identical results in the VASE analysis.

The VASE data are modeled by dividing the graded layer into $n = 30$ layers. The oxide thickness is found to be 43.0 Å ± 0.4 Å, and the unbiased estimator, σ, is 0.0202. The total layer thickness, D, is 0.97 μm ± 0.01 μm which is very close to the nominal values of 1.0 μm. The fitting, shown in Fig. 4, is excellent with the model diverging from the experimental data only in the low wavelength region of the Ψ spectra. The alloy composition at the substrate, x_0, is held constant in the analysis at 100%, the alloy composition at the ambient side of the graded layer is 58.7% ± 0.3%. This value differs from the nominal value of 50%. While it is possible that the nominal value is incorrect, the discrepancy is most likely due to residual strain in the graded layer. Because the graded layer is uncapped, the surface region of the layer is expected to be *coherently strained*. Using relaxed reference dielectric functions in the VASE analysis can cause the Si content to be overestimated up to 5% in strained Si_xGe_{1-x} layers on Si [11].

CONCLUSIONS

The energy shift algorithm has been applied to relaxed Si_xGe_{1-x} dielectric functions at discrete x values covering the complete compositional range. This allows the dielectric function for Si_xGe_{1-x} to be generated for all x, $0.0 \leq x \leq 1.0$. This in turn allows VASE to be used for the characterization of high Ge content Si_xGe_{1-x}/Ge heterostructures and also for Si_xGe_{1-x} graded alloy layers. VASE results for Si_xGe_{1-x}/Ge SL structures show excellent agreement with HRXRD results. VASE has also been successfully used to characterize a linearly graded Si_xGe_{1-x} layer.

ACKNOWLEDGEMENTS

The authors would like to thank G. E. Jellison for providing a diskette of his Si_xGe_{1-x} dielectric function database.

REFERENCES

[1] R. M. Sieg, S. A. Alterovitz, E. T. Croke, and M. J. Harrell, Appl. Phys. Lett. **62**, 1626 (1993).

[2] R. M. Sieg, S. A. Alterovitz, E. T. Croke, M. J. Harrell, M. Tanner, K. L. Wang, R. A. Mena, and P. G. Young, J. Appl. Phys. **74**, 586 (1993).

[3] G. E. Jellison, Jr., T. E. Haynes, and H. H. Burke, Opt. Mater. **2**, 105 (1993).

[4] P. G. Snyder, M. C. Rost, G. H. Bu-Abbud, J. A. Woollam, and S. A. Alterovitz, J. Appl. Phys. **60**, 3293 (1986).

[5] V. S. Speriosu and T. Vreeland, Jr., J. Appl. Phys. **56**, 1591 (1984).

[6] R. J. Hauenstein, B. M. Clemens, R. H. Miles, O. J. Marsh, E. T. Croke, and T. C. McGill, J. Vac. Sci. Technol. B **7**, 767 (1989).

[7] P. G. Snyder, J. A. Woollam, S. A. Alterovitz, and B. Johs, J. Appl. Phys. **68**, 5925 (1990).

[8] J. Humlíček, M. Garriga, M. I. Alonso, and M. Cardona, J. Appl. Phys. **65**, 2827 (1989).

[9] H. Yao, J. A. Woollam, P. J. Wang, M. J. Tejwani, and S. A. Alterovitz, Appl. Surf. Sci. **63**, 52 (1993).

[10] C. Pickering, R. T. Carline, D. J. Robbins, W. Y. Leong, S. J. Barnett, A. D. Pitt, and A. G. Cullis, J. Appl. Phys. **73**, 239 (1993).

[11] C. Pickering, R. T. Carline, D. J. Robbins, W. Y. Leong, A. D. Pitt, and A. G. Cullis, Proc. Soc. Photo-Opt. Instrum. Eng. **1985**, 414 (1993).

[12] P. Lautenschlager, M. Garriga, L. Viña, and M. Cardona, Phys. Rev. B **36**, 4821 (1987).

[13] E. S. Yang, *Microelectronic Devices* (McGraw-Hill, New York, 1988).

[14] F. H. Pollak, in *Strained-layer superlattices: Physics*, Vol. 32 of *Semiconductors and semimetals*, edited by T. P. Pearsall (Academic Press, San Diego, CA, 1990), Chap. 2, pp. 17–53.

[15] Y. Z. Hu, J.-T. Zettler, S. Chongsawangvirod, Y. Q. Wang, and E. A. Irene, Appl. Phys. Lett. **61**, 1098 (1992).